Comparison of One Step Implicit Integration Schemes for Creep Analysis Using the Finite Element Method

C. Nyssen, G. Panosyan, J. Beziat

NOVATOME, 20 av. E. Herriot, F-92350 Le Plessis-Robinson, France

A consequence of present-day severe nuclear plant operating conditions is the necessity to provide a more accurate description of the non-linear behaviour of the materials used for the components. In particular, structures can be subjected to non-negligible high temperature creep, which requires modelling.

Primary creep behaviour is characterized by a transient phase, with a decreasing strain rate, whereas secondary creep features a stationary phase with a constant strain rate.

Generally speaking, the creep behaviour of metals is a strong non-linear function of the stress and state variables, with leads to constitutive equations exhibiting stiff regime.

The finite element technique is now sufficiently developed to provide solutions to complex creep problems. Nevertheless, the choice of a precise and economical computational integration scheme to deal with creep phenomena remains a problem and very few results are available for primary creep.

Various one step implicit integration schemes are presented : the mid point rule, the purely implicit scheme and a non-iterative scheme, based on a first order linearization of the constitutive equations. The first two schemes can be proved to be unconditionally stable and the amplitude of the time step is only limited by the accuracy. The corresponding iterative schemes to solve the non-linear equilibrium equations obtained by the finite element method are derived in detail.

For primary creep, time hardening as well as strain hardening are considered. In the case of strain hardening, the rate of creep strain is assumed to be a function of the current stresses and the equivalent creep strain at the beginning of the time interval.

The convergence properties of the implicit schemes retained and the accuracy of the computed solutions are compared on a few examples using different time steps. Elastic and elasto-plastic cases are considered.

Guidelines for the choice of the step size are also discussed and shown to be efficient in the examples considered.

1. INTRODUCTION

Primary creep is of essential concern for Liquid Metal Fast Breeder Reactors (LMFBR) in which we are involved and this first stage of creep will be specially emphasized in this paper. The algorithms and integration schemes proposed can be applied straightforward to compute for secondary creep strain after a few simplifications.

The rapid variation of the strain rate at the beginning of the primary creep makes the computation delicate and needs refined computation algorithms. Three one step integration schemes were considered and will be discussed.

The guidelines for solving iteratively the non linear equilibrium equations obtained by the finite element method are given.

In the models selected, plastic and creep strains develop in conjunction, but the two phenomena are assumed to be entirely disconnected.

2. CREEP LAW

The interaction between plastic flow and creep is now well established /1/, but experimental data are not sufficient at the present time to qualify a mathematical model which could modelize such interaction. At first approximation ORNL recommendation will be retained /1/, neglecting such interactions.

For primary creep, Norton-Odqvist creep law will be considered ; i.e. the equivalent creep strain is given by :

$$\varepsilon^c = \alpha t^\beta \sigma^\delta \tag{1}$$

for $t < t_{pc}$. The end time of primary creep, t_{pc} , may be stated as

$$t_{pc} = \gamma \sigma^{-\eta} \tag{2}$$

All coefficients $\alpha, \beta, \delta, \gamma, \eta$ can be temperature dependent. For multiaxial cases, the creep flow law governing creep strain rate is given by /1, 3, 4/ :

$$\dot{\varepsilon}^c_{ij} = \frac{3}{2} \frac{\dot{\bar{\varepsilon}}^c}{\bar{\sigma}} t_{ij} , \tag{3}$$

Where t_{ij} is the stress deviator. The equivalent creep strain rate is obtained from (1) as :

$$\dot{\bar{\varepsilon}}^c = \alpha \beta t^{\beta-1} \sigma^\delta \tag{4}$$

The $\bar{\sigma}$ stress is the equivalent von Mises Stress.

In (4), the creep rates is only time dependent for a given stress level (time hardening model). Generally better results are obtained, in case of variable stresses, by using a strain hardening model. This can be obtained if, in equation (4), the time t is expressed in term of equivalent creep strain as given by equation (1) :

$$t = \left(\frac{\bar{\varepsilon}^c}{\alpha \bar{\sigma}^\delta} \right)^{1/\beta} \tag{5}$$

Strain hardening law for equivalent creep strain rate is then written

$$\dot{\bar{\varepsilon}}^c = (\alpha)^{1/\beta} \beta \left(\bar{\varepsilon}^c \right)^{1/\beta} \bar{\sigma}^{\delta/\beta} \tag{6}$$

In this model (6), the equivalent creep strain is directly expressed in terms of total creep strain components by /1, 3/

$$\dot{\bar{\varepsilon}}^c = \left(\frac{2}{3} \varepsilon^c_{ij} \varepsilon^c_{ij} \right)^{1/2} , \tag{7}$$

from which follows that in a general multiaxial case,

$$\bar{\varepsilon}^c \neq \int_t \dot{\bar{\varepsilon}}^c dt \tag{8}$$

The strain hardening model can lead to several difficulties in case of load reversals /1/, but such cases will not be considered.

3. SOLUTION ALGORITHMS

3.1. Relation between stress and strain increments

Only small strains will be considered in the following. Since creep-plasticity interaction are neglected, the total strain rate may be stated as :

$$\dot{\varepsilon}_{ij} = \dot{\varepsilon}^{e}_{ij} + \dot{\varepsilon}^{pl}_{ij} + \dot{\varepsilon}^{c}_{ij} + \dot{\varepsilon}^{th}_{ij} \tag{9}$$

where $\dot{\varepsilon}^{e}_{ij}$ is the elastic part of the deformation rate, $\dot{\varepsilon}^{pl}_{ij}$ the plastic part and $\dot{\varepsilon}^{th}_{ij}$ the thermal strain rate.

Using the classical Prandtl-Reuss-Von Mises plastic flow rules with isotropic hardening, for a given time increment Δt, stress and strain increments have to satisfy the linearized relations.

$$\Delta\varepsilon_{ij} = C^{-1}_{ijkl}\,\Delta\sigma_{kl} + \Delta\lambda a_{ij} + \Delta\varepsilon^{th}_{ij} + \Delta\varepsilon^{c}_{ij} \tag{10}$$

$$a_{ij}\Delta\varepsilon_{ij} = 4X\bar{\sigma}H'\Delta\lambda \tag{11}$$

Where H' is the strain hardening coefficient of the material, a_{ij} are the components of the normal to the intrinsic surface and X is the current elasticity limit.

As will be demonstrated in the following for the one step integration scheme, the creep strain increments can always be written in the from

$$\Delta\varepsilon^{c}_{ij} = \Delta\varepsilon^{co}_{ij} + F_{ijkl}\,(\sigma, t, \bar{\varepsilon}^{c})\,\Delta\sigma_{kl} \tag{12}$$

Using a generalized Hooke matrix defined by

$$C^{*}_{ijkl} = \left(C^{-1}_{ijkl} + F_{ijkl}\right)^{-1} \tag{13}$$

It follows from (10), (11) and (12) that the incremental stress-strain relation may be stated as

$$\Delta\sigma_{ij} = D^{*}_{ijkl}\,(\sigma, t, \bar{\varepsilon}^{c})\,\Delta\varepsilon^{mec}_{kl} \tag{14}$$

where the mechanical part of the strain increments are given by

$$\Delta\varepsilon^{mec}_{ij} = \Delta\varepsilon_{ij} - \Delta\varepsilon^{th}_{ij} - \Delta\varepsilon^{co}_{ij} \tag{15}$$

and with :

$$D^{*}_{ijkl} = C^{*}_{ijkl} - \frac{C^{*}_{ijrs}\,a_{rs}\,C^{*}_{klpq}\,a_{pq}}{4\bar{\sigma}H'X + a_{rs}C_{rspq}a_{pq}} \tag{16}$$

The tangential matrix D^{*}_{ijkl} is then identical to the classical one obtained for elastoplastic cases /2/ provided the general Hooke matrix (13) is used.

For non infinitesimal increments, the relation (14) must be rewritten as

$$\Delta\sigma_{ij} = \int D^{*}_{ijkl}\,(\sigma, t, \bar{\varepsilon}^{c})\,d\varepsilon^{mec}_{kl} \tag{17}$$

The numerical integration technique used to compute $\Delta\sigma_{ij}$ is given in details in /5, 2/. When creep takes place, the increments of stress in a given iteration are computed for fixed increments of total strains, thermal strain and creep strain.

Having derived the incremental stress-strain relation the non linear equilibrium equations of the finite element model can be easily established and solved by a classical Newton-Raphson method /5, 2/.

3.2. Computation of creep strain increments for a given Newton-Raphson iteration

Three one step integration schemes will be considered

3.2.1. Time Hardening cases

- One step implicit integrated scheme

In this first scheme all time depending quantities are supposed to vary linearly during the time step $\Delta t = t_2 - t_1$.

Creep rates are expressed through a first order development in terms of the variable increments and then integrated exactly on Δt. After some calculations one obtains easily :

$$\Delta\varepsilon^{c}_{ij} = \Delta\varepsilon^{co}_{ij} + F_{ijkl}\,\Delta\sigma_{kl} \tag{18}$$

with

$$\Delta\varepsilon^{Co}_{ij} = \frac{3}{2}\,\bar{\sigma}^{\delta-1}\left(M\,\frac{t_2^{\beta}-t_1^{\beta}}{\beta} + \Delta M f\right) t_{ij} \tag{19}$$

$$F_{ijkl} = \frac{3}{2}\, M\,\bar{\sigma}^{\delta-1} f\left(\delta_{ik}\delta_{jl} - \frac{1}{3}\delta_{kl}\delta_{ij} + \frac{3}{2}\,\frac{(\delta-1)}{\bar{\sigma}^{2}}\, t_{ij}\, t_{kl}\right) \tag{20}$$

where

$$M = \alpha\beta \tag{21}$$

$$f = \frac{(\beta+1)(t_1+\Delta t)^{\beta}\Delta t - (t_1+\Delta t)^{\beta+1} + t_1^{\beta+1}}{\Delta t\,\beta(\beta+1)} \tag{22}$$

δ_{ij} is the Kronecker tensor.

In this scheme, $\Delta\varepsilon^{Co}_{ij}$ and F_{ijkl} are constant and evaluated in term of the stresses in t_1. No iteration is thus needed if no plasticity occurs.

- Pure implicit and mid point schemes

Creep rates are supposed to be constant and equal to their values at $(\sigma_{ij} + \tau\Delta\sigma_{ij},\, t_1 + \tau\Delta t)$ where the parameter τ is equal to $1/2$ for the mid point scheme and to 1 for the pure implicit scheme

$$\Delta\varepsilon^{c}_{ij} = \frac{3}{2}\,(M+\tau\Delta M)(t_1+\tau\Delta t)^{\beta}(\bar{\sigma}+\tau\Delta\bar{\sigma})^{\delta-1}\,(t_{ij}+\tau\Delta t_{ij})\,\Delta t \tag{23}$$

Where stress variations occur during Δt, (23) is satisfied by successive iterations. At each iteration, the additional increments $d\Delta$ are given by

$$d\Delta\varepsilon^{c}_{ij} = d\Delta\varepsilon^{Co}_{ij} + F_{ijkl}\, d\Delta\sigma_{kl} \tag{24}$$

with

$$d\Delta\varepsilon^{Co}_{ij} = \frac{3}{4}\,(M+\tau\Delta M)(\bar{\sigma}^{*}+\tau\Delta\bar{\sigma})^{\delta-1}(t_1+\tau\Delta t)^{\beta-1}\Delta t \tag{25}$$

$$F_{ijkl} = \frac{3}{4}\,(M+\tau\Delta M)(\bar{\sigma}^{*}+\tau\Delta\bar{\sigma})^{\delta-1}(t_1+\tau\Delta t)^{\beta-1}\Delta t\ * \left(\delta_{ik}\delta_{jl} - \frac{1}{3}\delta_{kl}\delta_{ij} + \frac{3}{2}\,\frac{\delta-1}{(\bar{\sigma}^{*}+\tau\Delta\bar{\sigma})}\,(t_{ij}^{*}+\tau\Delta t_{ij})(t^{*}_{kl}+\tau\Delta t_{kl})\right) \tag{26}$$

The quantities are thus computed using the values of the stresses

$$\sigma_{ij} = \sigma^{*}_{ij} + \tau\Delta\sigma_{ij} \tag{27}$$

Where σ^{*}_{ij} are the stresses at the beginning of the whole increment and $\Delta\sigma_{ij}$ are the current stress increments at the beginning og the considered iteration,

$$\Delta\sigma_{ij} = \Sigma\, d\Delta\sigma_{ij} \tag{28}$$

The procedure is repeated until stabilization. Scheme (23) is unconditionally stable /6/.

3.2.2. Strain hardening cases

Now, creep ratios are defined in term of equivalent creep strain instead of time. The assumption is made that the equivalent creep strain at the beginning of the time interval has to be considered to define the strain hardening law. If in this case a pseudo-time t^{*} is defined as

$$t^{*} = \left(\frac{\varepsilon^{c}}{\alpha\bar{\sigma}^{\delta}}\right)^{1/\beta} \tag{29}$$

and $t_2 = t^{*} + \Delta t$, the preceding case is recovered.

The equivalent stress used in evaluation of t^{*} in (29) is based on the stresses at the beginning, the midden or at the end of time interval considered, depending of the integration scheme used.

4. CHOICE OF THE TIME INTEGRATION STEP Δt

4.1. Unconditionally stable schemes (with time hardening)

For this schemes, the precision alone governs the choice of the time step.

4.1.1. $\frac{\Delta\sigma}{\sigma} \sim 0$ on Δt

This is often the case for creep under constant loading. In one dimensional case, the truncature error is given by

$$e = \varepsilon^{c}_{t_2} - \varepsilon^{c}_{t_1} - \Delta t\,\alpha\beta(t_1+\tau\Delta t)^{\beta-1}(\sigma+\tau\Delta\sigma)^{\delta-1} \tag{30}$$

Using a Taylor serial expansion in Δt and $\Delta\sigma$ one obtains readily

$$\begin{aligned} e \simeq\ & \frac{\alpha\beta}{2}(\beta-1)\, t_1^{\beta-2}\sigma^{\delta}\Delta t^{2}(1-2\tau) \\ & + \frac{\alpha\beta}{6}(\beta-1)(\beta-2)\, t_1^{\beta-3}\sigma^{\delta}\Delta t^{3}(1-3\tau^{2}) \\ & + \alpha\delta t_1^{\beta}\sigma^{\delta-1}\Delta\sigma + \alpha\beta\delta\, t_1^{\beta-1}\sigma^{\delta-1}\Delta\sigma\Delta t\,(1-\tau) \end{aligned} \tag{31}$$

When $\frac{\Delta\sigma}{\sigma} \sim 0,$

$$e \simeq \frac{\alpha\beta}{2}(\beta-1)t_1^{\beta-2}\sigma^{\delta}\Delta t^2(1-2\tau) + \frac{\alpha\beta}{2}(\beta-1)(\beta-2)t_1^{\beta-3}\sigma^{\delta}\Delta t^3(1-3\tau^2) \qquad (32)$$

A good approximation for Δt is obtained if e is limited to a small fraction of the elastic strain.

$$|e| \leq \xi\frac{\sigma}{E} \qquad (33)$$

Good results were generally obtained using $\xi = 0.05$

- mid point rule

  Upper bound for Δt is given by

$$\Delta t \leq \left(\frac{24\,\xi\,t^{3-\beta}}{\sigma^{\delta-1}E\beta(\beta-1)(\beta-2)\alpha}\right) \qquad (34)$$

- Implicit scheme

  Upper bound for Δt is given by

$$\Delta t \leq \left(\frac{2\,\xi\,t^{2-\beta}}{\sigma^{\delta-1}E\beta(\beta-1)\alpha}\right) \qquad (35)$$

4.1.2. $\frac{\Delta\sigma}{\sigma}$ may not be neglected on time interval Δt (relaxation)

An estimation of the amplitude of Δt may be obtained by considering the relaxation equation of a simple viscoelastic solid /9/

$$\dot{\sigma} + \lambda(\sigma)\sigma = 0 \qquad (36)$$

Where

$$\lambda(\sigma) = \frac{E\dot{\varepsilon}^c}{\sigma} = E\alpha\beta t^{\beta-1}\sigma^{\delta-1} \qquad (37)$$

Should the parameter λ be constant in equation (37), solution of (36) would be

$$\sigma_{n+1} = e^{-\lambda\Delta t}\sigma_n \qquad (38)$$

Using (23) leads to

$$\sigma_{n+1} = \frac{1-(1-\tau)\lambda\Delta t}{1+\tau\lambda\Delta t}\sigma_n = A(\tau,\Delta t)\sigma_n \qquad (39)$$

A condition for $A(\tau,\Delta t)$ to be a good approximation of $e^{-\lambda\Delta t}$ is that

$$\lambda\Delta t \sim \zeta \qquad (40)$$

Where ζ is small as compared to one, thus if λ is considered independant of σ,

$$\Delta t \leq \frac{\zeta}{\lambda} = \frac{\zeta\sigma^{1-\delta}t^{1-\beta}}{\alpha\beta E} \qquad (41)$$

This will be used even for the real case, $\lambda = \lambda(\sigma)$, condition (41), is also given in /8/ for secondary creep and is generally more restrictive than (34) and (35).

4.2. One step implicit integrated scheme (time hardening)

Unconditional stability is not proven but in every computed cases, a good approximation for Δt is obtained through (34) and (41).

4.3. Choice of time step for strain hardening case

The same bounds (34), (35) and (41) on Δt are used, provided the time t is replaced by the pseudo-time defined in (29).

5. NUMERICAL EXAMPLES

The application discussed can be divided into 2 parts. The first one includes simple cases to validate the proposed creep algorithm implemented in our general purpose computer program /10/. The second part covers the elastoplastic creep analysis of an internally pressurized vessel /11/.

5.1. Creep at constant stress

An uniform biaxial state of stress /4/ is imposed on a specimen (figure 1). The solutions are computed for the three proposed scheme and using a constant time interval equal to 0.5 h. The implicit one step integrated scheme (18) gives the exact solution since the stresses are fixed (figure 1). The pure implicit and mid point schemes are then applied with Δt computed by (34) and (35) using $\xi = 0.05$. The results are given in figure 2 and demonstrate the interest of a good estimation of Δt.

5.2. Creep in a lead alloy internally pressurized vessel

A lead alloy vessel is submitted at 20°C to an internal pressure of 1.76 MN/m^2. Geometric and material data are given in figures 3 and 4. The pressure leads a pronounced plastification of the vessel. This loading is then sustained for 100 hours, during this hold time hoop and meridional strains are recorded . The creep law, adjusted in terms of differents results is given by (1) in (%),

with $\alpha = 1.0428.10^{-30}$ $\quad ((N/m^2)^{-4.07}\, h^{-0.436})$

$\beta = 0.436$

$\delta = 4.07$

In /11/ the coupling between plastic flow and creep is neglected.

The pressure of 1.76 MN/m^2 was first applied. In /11/, this involved 40 loading increments. Two elasto-plastic analysis were performed. In the first only four equal increments were applied.
Results are compared with the calculations and test results of /11/, in figure 5. Agreement between the solutions is excellent, which is quite outstanding, given the amplitude of the increments used. In the second analysis, the loading distribution was improved by application of the following load increments :

$$\Delta p_1 = 0.44 \text{ MN/m}^2 \quad ; \quad \Delta p_{2....11} = 0.132 \text{ MN/m}^2$$

The total hoop and meridional strains obtained by the two computations are compared in Table 1. The agreement between the solutions is quite good and demonstrates the capacity of NOVNL program /10/ to take large load increments into account in elasto-plastic analysis.

For the calculations of creep strains, we preferred as in /11/, the strain hardening method and adopted the mid point integration scheme. The time steps Δt were computed from (34) with $\xi = 0.05$ but with some of themadjusted to obtain results after 0.1 h, 1 h, 10 h and 100 h under creep. The Δt were taken as follows :

$$\Delta t_{1....11} = 0.01,\ 0.04,\ 0.05,\ 0.08,\ 0.4,\ 0.42,\ 1.40,\ 3.0,\ 4.6,\ 15.,\ 45 \text{ h}$$

In figure 6, the computed values of creep strain are compared to /11/ after 100 hours. Excellent agreement is observed for the hoop strains. For meridional strains the agreement on the meridional distribution of the equivalent creep strain can be considered as comparable to that of hoop strains, which is excellent.

In order to validate the time modelling, the program was re-run with each time step divided by two. The results do not differ significantly from those obtained previously and have not been included in figure 6. They are compared in Table 2.

REFERENCES

1. GREENSTREET, W.L., CORUM, J.M., PUGH, C.E. and LIU, K.C., "Currently recommended constitutive equations for inelastic design analysis of FFTF components", Oak Ridge National Laboratory, TM-3602.

2. NYSSEN, C., An efficient and accurate iterative method, allowing large incremental steps, to solve elasto-plastic problems, symposium on computational methods in non linear Structural and Solid Mechanics, Washington (1980).

3. RASHID, Y.R., "Analysis of two dimensional problems under simultaneous creep and plasticity" GEAP-10546, AEC Research and Development Report,January 1972.

4. DONEA, J. "The Application of computer Methods to Creep Analysis" in "Creep of engineering Materials and Structures", Ispra, November 1978.

5. NYSSEN, C. "Modélisation par éléments finis du comportement non linéaire de structures aérospatiales" Thèse de Doctorat, Université de Liège, 1979.

6. HUGUES, T.J.R. and TAYLOR, R.L., "Unconditionally stable algorithms for quasi-static elasto/visco plastic finite element analysis" Comp. and Struct. Vol.8, pp. 169-173, 1978.

7. CORMEAU, I., "Numerical stability in quasi-static elasto/visco-plasticity" Int. J. for Num. Meth. in Eng, Vol 9, pp 109-127, 1975.

8. SUTHERLAND W.H. "Finite element computer code for creep analysis" Nuclear Eng. and Design, 11, pp 269-285, 1969.

9. WILLIAM, K.J. "Numerical solution of inelastic rate process", Comp. and Struct, Vol 8, pp 511-531, 1978.

10. NOVNL, Analyse non linéaire statique et dynamique de structures, NOVATOME technical note MSD 80.039.

11. HYDE, T.H., WEBSTER, J.J. and FESSLER, H. "Comparison of finite element predictions of elasto-plastic and creep behaviour with experimental data from hemispherically ended, cylindrical pressure vessel models, Proc. of papers C 102/80, 1980.

Table 1. Pressurized vessel. Elasto-plastic analysis

Absc. (fig. 3)	4 increments				11 increments			
	Outer skin		inner skin		outer skin		inner skin	
	ε_z ($*10^{-4}$)	ε_θ	ε_z ($*10^{-4}$)	ε_θ	ε_z ($*10^{-4}$)	ε_θ	ε_z ($*10^{-4}$)	ε_θ
266.8	-3.35	2.65	33.89	5.01	-0.61	2.54	29.98	4.51
240.3	10.58	27.93	-1.73	34.80	7.89	27.26	-0.05	33.16
213.8	8.21	44.51	-6.15	54.96	7.72	45.42	-5.28	54.88
187.3	3.66	48.30	-2.78	59.56	4.66	50.56	-3.85	61.01
160.8	6.12	45.24	-4.22	55.85	6.15	46.37	-3.82	56.02
134.3	8.76	32.79	-0.84	40.77	6.33	32.06	· 0.58	38.92
108.0		13.36		17.79		12.79		16.52
83.6		4.47		6.70		4.50		6.41
58.8		4.05		5.03		4.14		5.04
34.1		5.03		5.93		5.08		5.91
9.3		5.54		6.41		5.54		6.38

Table 2. Pressurized Vessel. Creep strains (Hold time = 100 h)

Absc. (fig. 3)	11 time steps				22 time steps			
	Outer skin		inner skin		outer skin		inner skin	
	ε_z ($*10^{-4}$)	ε_θ	ε_z ($*10^{-4}$)	ε_θ	ε_z ($*10^{-4}$)	ε_θ	ε_z ($*10^{-4}$)	ε_θ
266.8	-2.28	3.40	29.40	3.38	-2.09	3.40	30.12	3.53
240.3	5.44	28.51	14.40	35.40	6.28	28.90	9.16	36.20
213.8	8.93	50.83	-8.16	64.23	9.03	52.20	-8.34	65.40
187.3	6.69	57.02	-9.01	74.11	6.25	60.20	-8.35	75.10
160.8	7.10	52.20	-7.01	66.62	7.07	54.20	-7.10	67.90
134.3	4.57	34.96	0.84	43.34	5.48	35.40	0.24	44.40
108.0		12.16		16.57		11.90		17.30
83.6		3.32		5.11		3.39		5.22
58.8		2.42		3.16		2.47		3.32
34.1		3.13		3.81		3.24		3.89
9.3		3.54		4.05		3.63		4.29

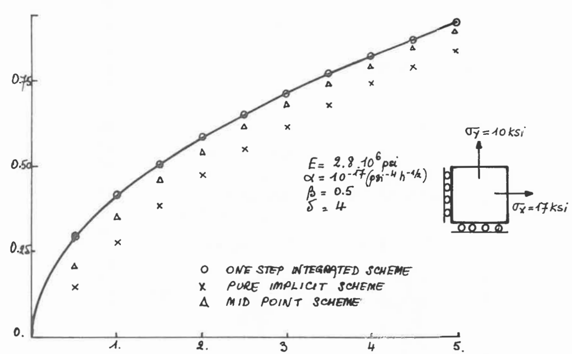

Figure 1 : Creep at constant stress (constant time interval)

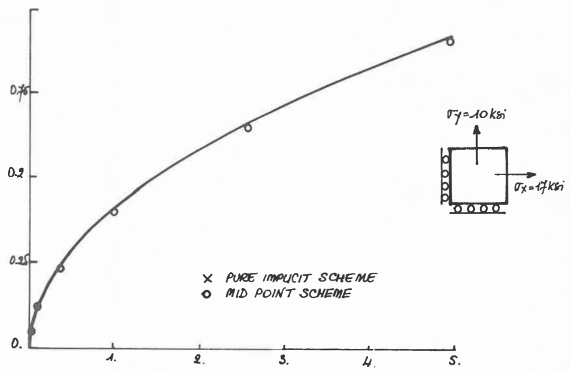

Figure 2 : Creep at constant stress (computed time interval)

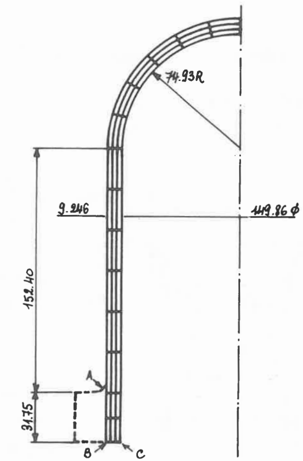

Figure 3 : Lead Alloy Vessel : Geometrical representation

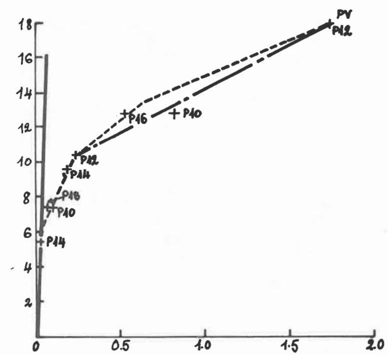

Figure 4 : Lead Alloy Vessel : Tensile curve

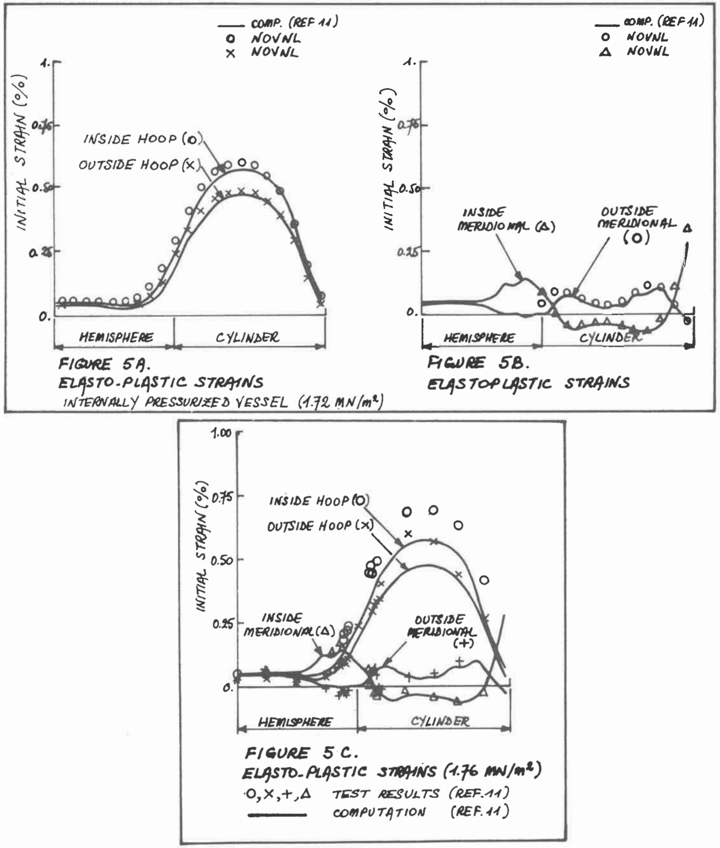

Figure 5 : Lead Alloy Vessel : Elasto-plastic strains (A, B, C)

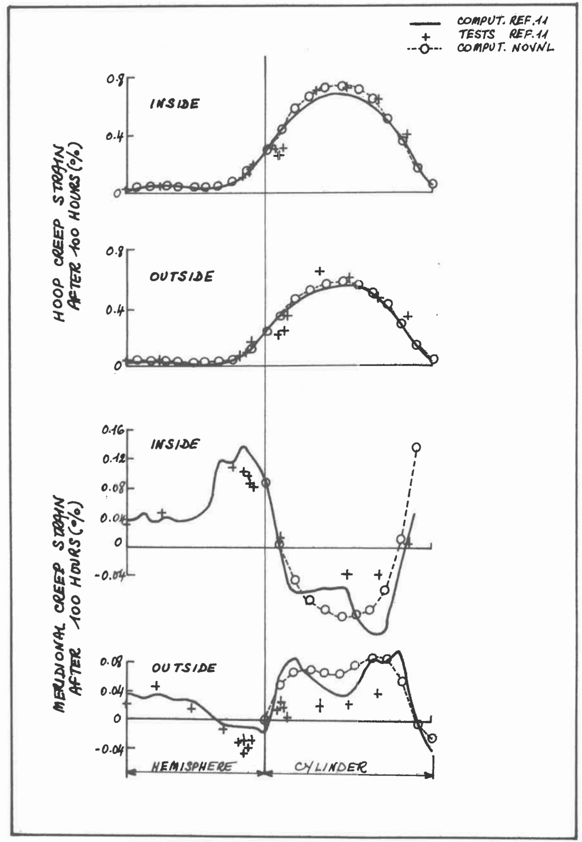

FIGURE 6. CREEP STRAIN AFTER 100 HOURS (%)

Figure 6 : Lead Alloy Vessel : Creep strain after 100 hours